Soliton generation and picosecond collapse in solid-state lasers with semiconductor saturable absorbers

V. L. Kalashnikov, D. O. Krimer, and I. G. Poloyko

International Laser Center, Building 17, 65 Skorina Avenue, Minsk 220027, Belarus

We study soliton generation, based on self-consistent field theory, in cw solid-state lasers with semiconductor saturable absorbers. Various soliton destabilizations, i.e., the switch from femtosecond to picosecond generation (picosecond collapse), an automodulation regime, breakdown of soliton generation, and hysteresis behavior, are predicted. It is shown that the third-order dispersion reduces the region in which the solitons exist and causes pulse oscillation and a strong frequency shift. © 2000 Optical Society of America
[S0740-3224(00)00504-X]

OCIS codes: 140.4050, 140.3430, 140.3580, 140.1540.

1. INTRODUCTION

Recent advances in ultrafast solid-state lasers have resulted in generation of sub-6-fs pulses directly from the cavity of Ti:sapphire lasers,[1] which is close to the theoretical limit for optical pulses. The key factor in mode locking in this case is fast optical nonlinearities, such as electronic nonlinearities, which are responsible, in particular, for self-phase modulation (SPM) and self-focusing.[2]

As has been shown, the generation of extremely short pulses in lasers with self-focusing or semiconductor saturable absorbers[3] is possible because of formation of a Schrödinger soliton. The relevant mechanism is the balance between SPM and group-velocity dispersion (GVD), which reduces the pulse duration and stabilizes it. This mechanism, termed soliton mode locking,[4] works with Kerr lensing or saturable absorption of the semiconductor, thus supporting the ultrashort pulse and preventing noise generation. However, the presence of dissipative laser factors, such as saturable gain and loss and frequency filtering, complicates the soliton dynamics, so various nonstationary regimes in Kerr-lens mode-locked lasers[5,6] and Q switching instability in cw lasers with semiconductor saturable absorbers[7] are possible. Until now a theoretical understanding of the issues mentioned above has been lacking and has presented challenges for investigators that can be of particular interest for the generation dynamics and control of pulse characteristics in the femtosecond region.

Here we present the results of our study of soliton generation in cw solid-state lasers with semiconductor saturable absorbers. The main focus of our investigation centered on the peculiarities of the transition between femtosecond (Schrödinger soliton) and picosecond generation. We demonstrate that such a transition is accompanied by threshold and hysteresis phenomena. Based on soliton perturbation theory, we performed numerical simulations of two different experimental situations. In the first one we varied the control parameters (dispersion or pump power); for every new value of a control parameter the laser was turned on afresh. In the second situation we continually varied the control parameters for an ultrashort pulse (the pulse was formed from the noise spike at start value of the control parameter). We demonstrate also that third-order dispersion destabilizes the soliton and produces a strong frequency shift of the generation wavelength with respect to the gain center.

2. MODEL

We analyzed the field evolution in a distributed laser system containing a saturable quasi-four-level gain crystal, a frequency filter, GVD and SPM elements, a two-level saturable absorber, and linear loss. We assumed that in a noncoherent approximation the action of the saturable absorber can be described by the operator $-\gamma \exp(-E/E_s)/(1 + \partial/\partial t)$,[8] where γ is the initial saturable loss, $E = \int_{-\infty}^{t} |a(t')|^2 \mathrm{d}t'$ is the energy fluence passed through the absorber to moment t, t is the local time, and E_s is the loss saturation energy fluence; expansion of the denominator into the time series in $\partial/\partial t$ is further supposed. We assume that the gain is saturated by the full pulse energy (i.e., we do not consider dynamic gain saturation). The ratio of the loss saturation energy to the gain saturation energy τ under assumption of equal cross sections of the generation mode at the semiconductor modulator and the Ti:sapphire active medium is 1.25×10^{-4} for $E_s = 100 \, \mu\mathrm{J/cm}^2$ (compare this with the value for semiconductor saturation energy reported in Ref. 3).

The evolution of generation field a obeys the following operator equation:

$$\frac{\partial a(z,t)}{\partial z} = \left\{ \alpha \exp(-\tau E) - \frac{\gamma \exp(-E)}{1 + \dfrac{\partial}{\partial t}} \right.$$

$$+ \left[\frac{1}{1 + \dfrac{\partial}{\partial t}} - 1 \right] - l + ik_2\frac{\partial^2}{\partial t^2} + k_3\frac{\partial^3}{\partial t^3}$$

$$\left. - i\beta|a(z,t)|^2 \right\} a(z,t), \tag{1}$$

where z is the longitudinal coordinate normalized to the cavity length, or transit number, α is the saturated gain, l is the linear loss, $k_{2,3}$ are the second- and third-order dispersion coefficients, respectively, and the energy fluence is normalized to E_s. The time is normalized to the inverse bandwidth of the absorber $1/t_a$. With this normalization the SPM coefficient β is $2\pi n_2 LE_s/\lambda n t_a$, where L is the length of the crystal, n and n_2 are the linear and nonlinear coefficients of refractivity, respectively, and λ is the generation wavelength. The term in brackets in Eq. (1) stands for the frequency filtering. The transmission band of the filter and the absorption band of semiconductor were assumed to coincide. An expansion of Eq. (1) to second order in $\partial/\partial t$ results in a nonlinear Landau–Ginzburg equation,[4,8] which we do not write out here because of its complexity.

Because an exact general solution of Eq. (1) is unknown, we sought an approximate quasi-soliton solution in the form

$$a(z,t) = a_0\frac{\exp[i\omega(t - z\delta) + i\varphi z]}{\cosh[(t - z\delta)/t_p]^{1+i\Psi}},$$

where a_0 is the amplitude, t_p is the width, ω is the frequency mismatch from filter band center, Ψ is the chirp, and φ and δ are the phase and time delays, respectively, after the full cavity round trip. In the frame of an aberrationless approach,[9] the substitution of this solution into Eq. (1) with a following expansion in t yields the following set of ordinary differential equations for the evolution of the pulse parameters:

$$\frac{da_0}{dz} = a_0\left[\alpha \exp\left(-\frac{\tau a_0^2}{v}\right) + (1 - \omega^2 - v^2)\gamma \exp\left(-\frac{a_0^2}{v}\right) \right.$$

$$\left. - l + k_2\Psi v^2 - \omega^2 - v^2 - 3k_3\omega v^2\Psi \right],$$

$$\frac{d\omega}{dz} = (\Psi a_0^2\omega^2 + a_0^2\omega - 2v^2\omega - 2v^2\omega\Psi^2$$

$$- \Psi a_0^2)\gamma \exp\left(-\frac{a_0^2}{v}\right) - 2v^2\omega\Psi^2 - 2v^2\omega$$

$$- \Psi a_0^2\tau\alpha \exp\left(-\frac{\tau a_0^2}{v}\right) - 3k_3v^4\Psi(\Psi^2 + 1),$$

$$\frac{dv}{dz} = \frac{1}{2v^2}(a_0^4v^2 + 2v^4\Psi^2 - a_0^4 + a_0^4\omega^2 + 2a_0^2v^2$$

$$- 4a_0^2\omega v^2\Psi - 4v^4)\gamma \exp\left(-\frac{a_0^2}{v}\right)$$

$$- \frac{a_0^4\tau^2\alpha}{2v^2}\exp\left(-\frac{\tau a_0^2}{v}\right) + 3k_2v^2\Psi + v^2\Psi^2$$

$$- 2v^2 - 9k_3\omega\Psi v^2,$$

$$\frac{d\Psi}{dz} = \frac{1}{v^2}(4a_0^2\omega v^2 + a_0^4\Psi + 4a_0^2\omega v^2\Psi^2 - 2v^4\Psi$$

$$- \Psi a_0^4\omega^2 - a_0^4\omega - 2v^4\Psi^3)\gamma \exp\left(-\frac{a_0^2}{v}\right)$$

$$+ \frac{\Psi\alpha a_0^4\tau^2}{v^2}\exp\left(-\frac{\tau a_0^2}{v}\right) - 2a_0^2\beta - 2v^2\Psi$$

$$- 4k_2v^2\Psi^2 - 2v^2\Psi^3 - 4k_2v^2$$

$$+ 12k_3\omega v^2(\Psi^2 + 1), \tag{2}$$

where $v = 1/t_p$ is the inverse pulse width, and the solutions for time and phase delays are, respectively,

$$\delta = [a_0^2(\omega^2 + v^2 - 1) - 2v^2\omega\Psi]\gamma \exp\left(-\frac{a_0^2}{v}\right)$$

$$- 2\omega\Psi v^2 - 2k_2\omega v^2 + k_3v^2(5v^2 + 3\omega^2 - 3v^2\Psi^2)$$

$$- a_0^2\tau\alpha \exp\left(-\frac{\tau a_0^2}{v}\right),$$

$$\varphi = [a_0^2\omega(\omega^2 + v^2 - 1) + v^2\Psi(v^2 - 2\omega^2)]\gamma$$

$$\times \exp\left(-\frac{a_0^2}{v}\right) + k_3v^2\omega(2v^2 + 2\omega^2 - 3v^2\Psi^2)$$

$$+ k_2v^2(v^2 - \omega^2) + \Psi v^4 + \beta a_0^2v^2$$

$$- 2\omega^2\Psi v^2 - \omega\tau\alpha a_0^2 \exp\left(-\frac{\tau a_0^2}{v}\right).$$

Assuming that the pulse width is much shorter than the cavity period T_{cav}, the equation for the gain evolution is

$$\frac{d\alpha}{dz} = (\alpha_m - \alpha)P - \frac{2\alpha\tau a_0^2}{v} - \frac{\alpha}{T_g}, \tag{3}$$

where $P = (\sigma T_{cav}I_p/h\nu)$ is the dimensionless pump intensity, σ is the absorption cross section at the pump wavelength, $h\nu$ is the energy of the pump photon, and α_m is the maximal gain at the full population inversion. $P = 10^{-4}$ corresponds to a pump power of 1 W for a 100-μm-diameter pump mode.

The steady-state solution of Eqs. (2) and (3) describes the generation of stable ultrashort pulses. The system of Eqs. (2) and (3) was solved by the forward Euler method with $\sim10^6$ iterations and an accuracy of $\sim10^{-6}$.

3. DISCUSSION

First we study the situation when for each new value of control parameter the generation is formed starting from the noise spike as an initial approximation.

The normalized width of the stable pulse versus the GVD coefficient is presented in Fig. 1 for several values of SPM. It is well known that in solid-state lasers, unlike in dye lasers, mode locking with a slow saturable absorber is hindered by inefficient dynamic gain saturation (a small τ in our notation) but at the same time the presence of SPM can provide stable soliton mode locking.[4] As expected, our calculations confirmed this conclusion about the absence of stable mode locking for the situation with no SPM present in the system. However, introducing SPM stabilizes the picosecond generation (region A in Fig. 1) because of the action of negative feedback [7,8] (top-left segment of curve 1 in Fig. 2). The mechanism of this feedback is as follows: An increased pulse intensity causes stronger chirping, i.e., a wider pulse spectrum and, consequently, a higher loss at the bandwidth-limiting element; a decreased intensity, however, minimizes the chirp and the spectral width, reducing the loss at the spectral filter.

There is a section of curves 1–4 (Figs. 1 and 2) where the Schrödinger soliton exists within a limited window of negative dispersion. In this case the pulse durations lie in the femtosecond region, with the minimum close to zero GVD. Now the pulse intensities are much higher and the chirp is very small (central part of curve 1 in Fig. 2). Calculations showed that, contrary to the case of picosecond pulse durations and the situation with nonzero third-order dispersion, here the soliton frequency does not shift from the filter band center and its energy is equal to the critical energy for the first-order Schrödinger soliton $E = (2|k_2|)/(t_p\beta)$.
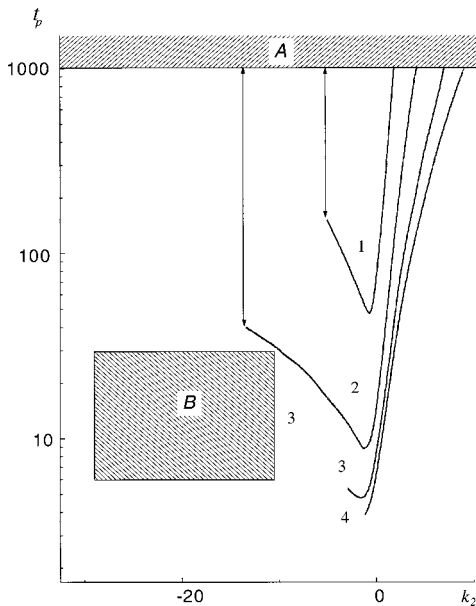

Fig. 2. Chirp Ψ versus GVD coefficient k_2. The parameters correspond to those of Fig. 1. Curves 3 and 4 exist for $k_2 \geqslant -3$ and $k_2 = -1$, respectively.

Fig. 3. Peak intensity I normalized to $E_s t_a^{-1}$ versus round-trip number z. $k_2 = -20$, $k_3 = 0$, $P = 5 \times 10^{-4}$, $\beta = 0.05$.

At some negative GVD the switch from the femtosecond to the picosecond regime (picosecond collapse, marked by an arrow; see curve 1 in Fig. 1) takes place. Formally, these two types of ultrashort generation correspond to domination of either nondissipative (Schrödinger soliton generation) or dissipative (picosecond generation) terms in Eq. (1), respectively.

For the stronger SPM (curve 2 in Fig. 1), the interval of GVD where femtosecond generation takes place broadens, accompanied by shortening of the pulse width (cf. curves 1 and 2 in Figs. 1 and 2). As can be seen, the picosecond collapse occurs now at much higher (in both negative and positive regions) dispersions.

Further increasing SPM transforms the character of soliton destabilization (curve 3 in Fig. 1). In this case, femtosecond generation is possible only near zero dispersion; the higher negative GVD destroys the solitonlike pulse (discontinuity of curve 3). At the left of the region where no quasi-soliton solution for Eq. (1) exists there is a region of pulse automodulational instability (region B). Here the pulse parameters oscillate with the period of ~ 100 cavity round trips (~ 1 μs), as illustrated in Fig. 3. The oscillating pulse is of the quasi-Schrödinger soliton type, with a small chirp (region B in Fig. 2) and a small frequency shift.

Fig. 1. Pulse width t_p versus GVD coefficient k_2 (time is normalized to t_a). Region A, picosecond generation; region B, auto-oscillation regime for parameters of curve 3. $P = 5 \times 10^{-4}$, $\alpha_m = 0.5$, $t_a = 2.5$ fs, $T_g = 3$ μs, $T_{cav} = 10$ ns, $l = 0.01$, $\gamma = 0.05$, $k_3 = 0$. $\beta = 1, 0.001; 2, 0.01; 3, 0.05; 4, 0.1$.
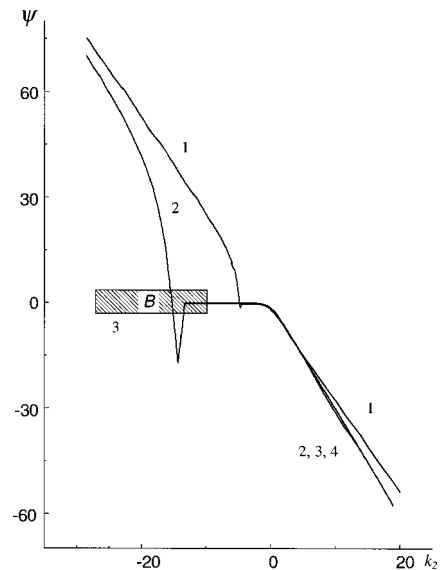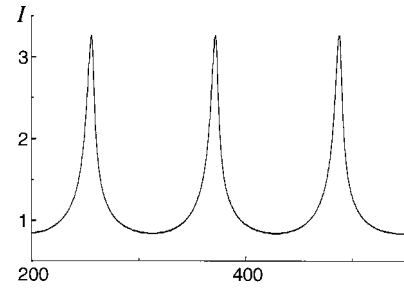
A further increase of SPM (curve 4 in Fig. 1) reduces the interval of quasi-soliton existence. Comparing curves 1–4 of Fig. 1, one may conclude that the optimal amount of SPM exists, providing femtosecond generation in the widest interval of GVD.

Let us consider pump intensity P, which is another control parameter of the system switching between picosecond (ps) and femtosecond (fs) regimes. As can be seen from Fig. 4 (triangles and arrow 1), the increase of the pump intensity switches the laser from ps to fs generation. This occurs when the pump intensity and, consequently, the generation pulse intensity become high enough for SPM to compensate for the GVD.

We investigate the dependence of system behavior on control parameters (pump, GVD) in two cases. First we calculate the pulse characteristics at some value of a control parameter and then turn off the mapping procedure [Eqs. (2) and (3)] so that for another value of the control parameter we take the noise spike as the initial value of Eqs. (2) and (3). This case is depicted in Figs. 1 and 2 and by triangles in Fig. 4. The second case corresponds
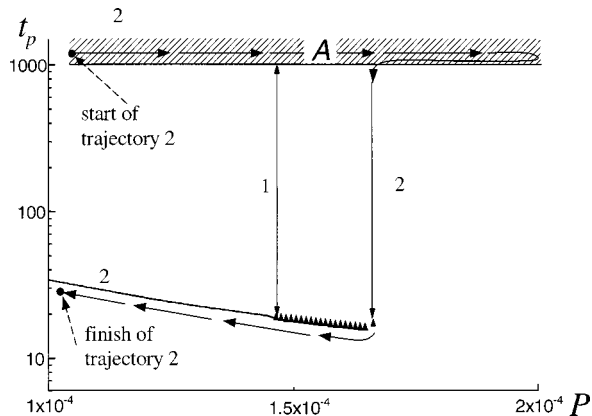

Fig. 4.   Pulse width t_p versus pump intensity P (time is normalized to t_a). Arrow l, switch between ps and fs generation for the regime depicted by triangles. Trajectory 2 (and corresponding arrow 2), variation of the pump for the previously formed pulse (i.e., for the pulse that is formed at $P = 10^{-4}$). $k_2 = -10$, $k_3 = 0$, $\beta = 0.1$; other parameters correspond to those of Fig. 1.
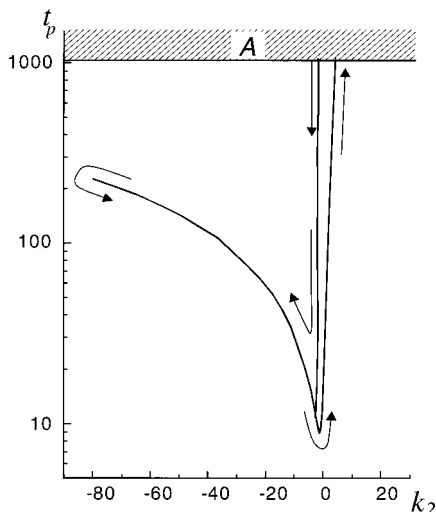

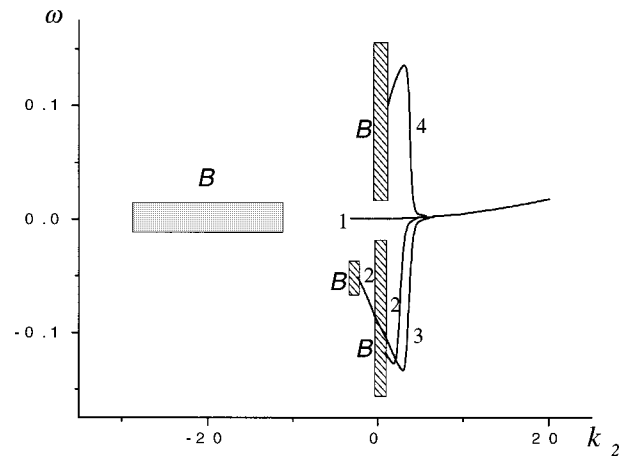Fig. 5.   Pulse width t_p versus GVD coefficient k_2. Parameters correspond to those of curve 2 of Fig. 1.

Fig. 6.   Frequency shift ω versus GVD coefficient k_2. Parameters correspond to those of curve 3 of Fig. 1. $k_3 = 1, 0; 2, -5; 3, -10; 4, 10$. The left-most region B (depicted in solid gray) corresponds to all presented parameters.

to the ultrashort pulse, which is produced by mapping at some value of the control parameter and then beginning the smooth variation of this parameter. This case is depicted in Figs. 4 and Fig. 5.

As can be seen from Fig. 4, the dependence of the pulse duration on the pump intensity demonstrates a hysteresis behavior. The pump variation from small to large values and vice versa produces the following sequence of generation regimes (trajectory 2 in Fig. 4): the pump increase from 10^{-4} to 2×10^{-4} does cause the system to switch from ps to fs generation; however, the subsequent pump decrease from 2×10^{-4} to 1.67×10^{-4} switches the system to the fs regime. The range of fs generation in terms of P (solid curve) is greater than for the case denoted by triangles, which was plotted analogously to the curves of Figs. 1 and 2. If the trajectory starts from large P, the ps regime is not operative, and the fs soliton forms at $P \approx 1.67 \times 10^{-4}$ (solid curve). In this case, the interval in which a soliton exists is wider than for the regime denoted by the triangles.

The system demonstrates hysteresis behavior as GVD varies, too (Fig. 5): Changing the GVD from negative values to zero and then to positive values does not cause a switch from ps to fs generation. On the other hand, when we move from positive values of dispersion to negative ones and back we can see the dramatic change in the system's behavior. The decrease of GVD starting from the positive values, where the ps generation takes place, causes an abrupt switch to fs generation near zero GVD. Comparing curve 2 in Fig. 1 and the curve in Fig. 5 that was plotted for the same parameters but for different physical situations (described above), one may conclude that the region of soliton existence is greater in terms of GVD for the latter case (when we change GVD for the previously formed pulse) than for the former (when the pulse is formed from the noise spike). The switch from fs (Schrödinger soliton) to ps generation on inverse movement along the GVD axis takes place at another value of GVD, thus producing a hysteresis feature (see Fig. 5).

In as much as Schrödinger soliton formation occurs at a small negative GVD, the contribution of third-order dispersion k_3 in this region may be essential. The presence

of $k_3 \neq 0$ gives rise to the following effects: (1) a strong pulse frequency shift, which depends on the sign of k_3 (cf. curves 2–4 with and curve 1 in Fig. 6), arises; (2) the region of fs generation narrows; and (3) an additional destabilizing factor, frequency shift oscillations, appears (regions B for curves 2–4 in Fig. 6).

4. CONCLUSION

In summary, based on the self-consistent field theory, we have investigated the characteristics of a Schrödinger soliton in a cw solid-state laser with a semiconductor saturable absorber. We demonstrated numerically that the formation of the soliton has a threshold character, so, together with first (free-running) and second (mode-locking) thresholds, a threshold of femtosecond generation exists. Three main destabilization situations were demonstrated: the switch to picosecond generation (picosecond collapse), the switch to automodulation mode, and the breakdown of a solitonlike pulse. The switch between ps and fs generation has a hysteresis character. The contribution of high-order GVD reduces the interval of quasi-soliton existence and gives rise to a frequency shift and pulse destabilization.

Our results may be useful for the design of self-starting cw solid-state lasers with controllable ultrashort pulse characteristics.

ACKNOWLEDGMENT

V. L. Kalishnikov's e-mail address is vkal @ilc.unibel.by.

REFERENCES

1. D. H. Sutter, G. Steinmeyer, L. Gallmann, N. Matuschek, F. Morier-Genoud, and U. Keller, "Semiconductor saturable-absorber mirrors assisted Kerr-lens mode-locked Ti:sapphire laser producing pulses in the two-cycle regime," Opt. Lett. **24**, 631–633 (1999).
2. H. Haus, J. G. Fujimoto, and E. P. Ippen, "Analytic theory of additive pulse and Kerr lens mode locking," IEEE J. Quantum Electron. **28**, 2086–2095 (1995).
3. U. Keller, K. J. Weingarten, F. X. Kärtner, D. Kopf, B. Braun, I. D. Jung, R. Fluck, C. Hönninger, N. Matuschek, and J. A. der Au, "Semiconductor saturable absorbers mirrors (SESAM's) for femtosecond to nanosecond pulse generation in solid-state lasers," IEEE J. Sel. Top. Quantum Electron. **2**, 435–451 (1996).
4. F. X. Kärtner, I. D. Jung, and U. Keller, "Soliton mode-locking with saturable absorbers," IEEE J. Sel. Top. Quantum Electron. **2**, 540–555 (1996).
5. S. R. Bolton, R. A. Jenks, C. N. Elkinton, and G. Sucha, "Pulse-resolved measurements of subharmonic oscillations in a Kerr-lens mode-locked Ti:sapphire laser," J. Opt. Soc. Am. B **16**, 339–344 (1999).
6. V. L. Kalashnikov, I. G. Poloyko, V. P. Mikhailov, and D. von der Linde, "Regular, quasi-periodic and chaotic behavior in cw solid-state Kerr-lens mode-locked lasers," J. Opt. Soc. Am. B **14**, 2691–2695 (1997).
7. C. Hönninger, R. Paschotta, F. Morier-Genoud, M. Moser, and U. Keller, "Q-switching stability limits of continuous-wave passive mode locking," J. Opt. Soc. Am. B **16**, 46–56 (1999).
8. V. L. Kalashnikov, D. O. Krimer, I. G. Poloyko, and V. P. Mikhailov, "Ultrashort pulse generation in cw solid-state laser with semiconductor saturable absorber in the presence of the absorption linewidth enhancement," Opt. Commun. **159**, 237–242 (1999).
9. A. M. Sergeev, E. V. Vanin, and F. W. Wise, "Stability of passively modelocked lasers with fast saturable absorbers," Opt. Commun. **140**, 61–64 (1997).